RSC Advances

PAPER

View Article Online
View Journal | View Issue

Cite this: *RSC Adv.*, 2020, **10**, 35407

Instant and quantitative epoxidation of styrene under ambient conditions over a nickel(II) dibenzotetramethyltetraaza[14]annulene complex immobilized on amino-functionalized SBA-15

Mohamed Abboud, *[a] Nabil Al-Zaqri,[b] Taher Sahlabji,[a] Murad Eissa,[a] Ahmed T. Mubarak,[a] Radhouane Bel-Hadj-Tahar,[ac] Ali Alsalme,[b] Fahad A. Alharthi,[b] Amjad Alsyahi[b] and Mohamed S. Hamdy[a]

Received 23rd August 2020
Accepted 15th September 2020

DOI: 10.1039/d0ra07244c

rsc.li/rsc-advances

Nickel(II)dibenzotetramethyltetraaza[14]annulene complex (Nitmtaa) was synthetized and immobilized on post amino-functionalized SBA-15 (N-SBA-15) to obtain a stable and reusable nanocatalyst named as Nitmtaa@N-SBA-15. Here (3-aminopropyl)triethoxysilane (APTES) was first grafted on the surface SBA-15, then Nitmtaa was added and coordinated on the silica surface *via* APTES amine groups. The structure and morphology, and thermal stability of the prepared nanocatalyst was investigated using SEM, HR-TEM, BET, FT-IR, powder XRD, and TGA. HR-TEM and XRD results revealed a high dispersion of Nitmtaa on the SBA-15 surface. The catalytic activity of this nanocatalyst was evaluated in the epoxidation of styrene, under ambient conditions, using *meta*-chloroperoxybenzoic acid (*m*-CPBA) as the oxygen donor. This nanocatalyst showed an immediate and quantitative epoxidation of styrene with high turn-over-frequency ~31.58 s^{-1}. Moreover, the superior catalytic activity and high stability of Nitmtaa@N-SBA-15 could be maintained after four successive cycles. A possible reaction mechanism is also proposed.

1. Introduction

Epoxides are particularly important raw materials and synthesis intermediates and have been vastly used in organic and pharmaceutical synthesis, and perfume processing.[1–4] Styrene oxide (STO) is one of the most important epoxides, and is used as an intermediate precursor for a huge variety of fine chemicals.[5]

The conventional processes for the epoxidation of styrene use organic peracids or employ addition of hypochlorous acid (HOCl) followed by dehydrochlorination using a base.[6] These homogeneous methods are however not eco-friendly as they produce a large amount of chlorinated by-products such as acid, and calcium chloride waste.

In recent years, the heterogeneous catalytic epoxidation of styrene has attracted many researchers' attention as an important route to produce STO. Transition metal-based catalysts, such as transition metal ions, transition metal-oxo and -peroxo complexes, organotransition metal complexes (OTMC), or transition-metal surfaces are the most investigated catalysts for the epoxidation of styrene.[7] In recent years, many efforts have been devoted to developing simple and efficient routes for the epoxidation of styrene by applying efficient and highly effective catalysts. OTMC have shown significant efficiency towards the catalytic epoxidation of styrene. Most of OTMC have been evaluated in epoxidation of styrene are Schiff base metal complexes and metallo-porphyrins, using various oxidants such as H_2O_2, O_2, *tert*-butyl hydroperoxide *t*-BuOOH, iodosylbenzene PhIO and *m*-CPBA.[7–10]

Dibenzotetraaza(14)annulene complexes derivatives have been used as catalysts in many reactions including the hydroxylation and epoxidation of alkenes.[11,12] They are interesting macrocycles for both practical and theoretical reasons. Their structure is similar to many important natural macrocycles or enzymes, such as peroxidases, Fator 430 (F-430), chlorophylls, catalase, cytochromes P-450, oxygenases and, oxygen transferring proteins such as hemoglobin and myoglobin.[11,13] In addition dibenzotetraaza[14] annulene framework is synthetically accessible, and its structure is similar to porphyrins, with co-planar four donor nitrogen atoms, substantial unsaturation and delocalisation. Unlike porphyrins, dibenzotetraaza(14)annulenes are Hückel anti-aromatic, and adopt saddle-like or nearly planar conformations, depending on the ring substituents. Moreover, metal complexes of porphyrins have excellent catalytic activity, but practical applications have been obstructed by their multistep synthesis, and low chemical

[a]*Catalysis Research Group (CRG), Department of Chemistry, College of Science, King Khalid University, P.O. Box 9004, Abha 61413, Saudi Arabia. E-mail: Abboud_med@yahoo.fr; mabboud@kku.edu.sa; Tel: +966 53 48 46 782*

[b]*Department of Chemistry, College of Science, King Saud University, P.O. Box 2455, Riyadh 11451, Saudi Arabia*

[c]*Photovoltaic Laboratory, Research and Technology Center of Energy, Borj-Cedria Science and Technology Park, BP 95, 2050 Hammam-Lif, Tunisia*

stability. In addition, porphyrins tend to deactivate *e.g.* by oxidative degradation, pyrrole unit alkylation or by comproportionation.[14]

Notably, while Nitmtaa was already prepared and characterized by Jaeger (1969) and Goedken (1973)[15–17] to the best of our knowledge, it has never been employed successfully as a catalyst until now. Caiut *et al.* reported the encapsulation of Nitmtaa in alumina matrix by sol–gel process to investigate the epoxidation of cyclooctene using PhIO as oxygen donor. However, the reaction was slow with low conversion and high Nitmtaa leaching.[18]

The utilisation of efficient OTMC catalysts in homogeneous conditions or physically incorporated in solid matrix has many drawbacks, such as no reusability, leaching and limited activity to a few turnovers. In contrast, the heterogenization of these catalysts by incorporating them in a solid matrix *via* chemical bonds will increase their stability, facilitate their separation, and make their reusability possible. For these advantages, various supports have been used in the literature such as mesoporous silica,[19–22] nanoporous carbon,[23] zeolites,[24] polymers,[25] clays[26–29] and resins.[30] In addition, the porous solid matrixes with high surface area and pore size, such as mesoporous silica SBA-15, allow good diffusion of reactants to the interior active sites of the catalyst without using swelling media.[31,32] However, the heterogenization of an efficient, stable, and reusable catalyst using a simple procedure to obtain high yield and selectivity in mild conditions is still attracting the attention of research activities.

Recently, we reported the synthesis, characterisation and catalytic activity of TUD-1 supported Ni nanoparticles (Ni-TUD-1). This nanocatalyst exhibited an immediate and quantitative conversion of cyclohexene to cyclohexene oxide in ambient conditions using *m*-CPBA as the oxygen donor. However, the catalytic activity of Ni-TUD-1 was decreased dramatically after four cycles, due to leaching of Ni nanoparticles from the support (TUD-1).[33]

Herein, we report the successful synthesis, characterization, and catalytic activity evaluation of Nitmtaa immobilized on amino-functionalized mesoporous silica SBA-15 (N-SBA-15) as a new nanocatalyst, which named Nitmtaa@N-SBA-15 (Scheme 1). APTES was grafted in SBA-15 surface and Nitmtaa immobilized on N-SBA-15 surface *via* coordinate bond with NH_2 of APTES. The obtained nanocatalyst was characterized by TEM, SEM, FT-IR, BET, TGA and XRD. The catalytic activity performance of this new nanocatalyst was investigated in the epoxidation of styrene in ambient conditions using *m*-CPBA as oxygen donor.

2. Experimental section

2.1 Materials

Nickel acetate tetrahydrate ($Ni(OAc)_2 \cdot 4H_2O$), *o*-phenylenediamine, acetylacetone, SBA-15, 3-aminopropyltriethoxysilane (APTES), styrene (99%), styrene oxide (97%), *meta*-chloroperoxybenzoic acid (*m*-CPBA) (99%), dichloromethane (99.8%), acetonitrile (99.9%), ethanol (99.8%), toluene (99.5%), were purchased from Sigma Aldrich. All reagents were of analytical grade, and used without further purification.

2.2. Methods

The morphology of the prepared nanocatalyst was investigated using a scanning electron microscopy (SEM; Philips EM 300) (Siemens Autoscan, Munchen, Germany). Transmission electron microscopy (TEM) micrographs were obtained using FEI Tecnai G2 F30 TEM operating at 200 kV. TEM images were captured using a CCD camera. TEM samples were prepared by suspending the material in ethanol using bath sonication for few minutes, applying a drop of the resulting suspension onto a carbon coated copper grids with lacey carbon (Ted Pella Inc.) and then leaving it to dry at room temperature (r.t. ~22 °C). FT-IR spectra were collected on FT spectrometer (Bruker Vector 22, Ettlingen, Germany) with a wavelength range 4000 to 500 cm^{-1}. Shimadzu Lab-XRD-6000 with CuK_α radiation and a secondary monochromator was used to measure the X-ray diffraction pattern. The thermal stability of the obtained material was investigated under air using a STAR^e System thermogravimetric analyzer (TGA) operating at rate 50 mL min^{-1} of air. In this process, around 20.0 mg sample was placed in a platinum crucible and heated at 15 K min^{-1} from 25 to 900 °C. The specific surface area, pore volume, pore size, and pore-size distribution of the heat-treated powder samples were determined by using a Micrometrics ASAP 2010 apparatus (Norcross, GA).

The epoxidation reaction was monitored by Shimadzu GC-17A gas chromatography (GC), equipped with flame ionization detector and RTX-5 column, 30 m × 0.25 mm, 1 μm film thickness. Helium was used as carrier gas at flow rate of 0.6 mL min^{-1}. Samples were withdrawn from the reaction mixture periodically. Injection volume was 1 μL, and total flow was 100 mL min^{-1}. Oven temperature was initiated at 100 °C for 2 min up to 130 °C at a rate of 15 °C min^{-1} held for 2 min, then increased to 150 °C at a rate of 2 °C min^{-1} held for 2 min. The injector temperature was 160 °C and the detector temperature was 200 °C. The amount of Ni in the solid catalyst and leached form the catalyst to the filtrate was measured using Varian model SpectrAA-220 flame atomic absorption spectrometer (Mulgrave, Vic., Australia) equipped with a deuterium background corrector. A nickel hollow cathode lamp was used as light source and was operated at 15 mA.

2.2.1 Measurement of Ni% in the solid catalyst and in the filtrate (leaching) using atomic absorption spectrometer (AAS). About 25 mg of the catalyst was weighed and placed in a Teflon cup, then 8 mL of the digestion mixture of HCl : HNO_3 : HF (5 : 2 : 1 v/v/v) were added. The Teflon cup was fitted in the Anton Paar microwave digestion system. Three steps of microwave program were applied as follows: (i) 5 min rump to 120 °C and 600 W; (ii) 40 min hold at 600 W; (iii) 15 min cooling at 0 W. Samples were filtered after digestion using filter paper no. 42. The mixture volume was then completed to a 100 mL. The liquid samples (filtrate) were directly measured without digestion.

The measurements of Ni% were carried out by Varian model SpectrAA-220 flame atomic absorption spectrometer mentioned

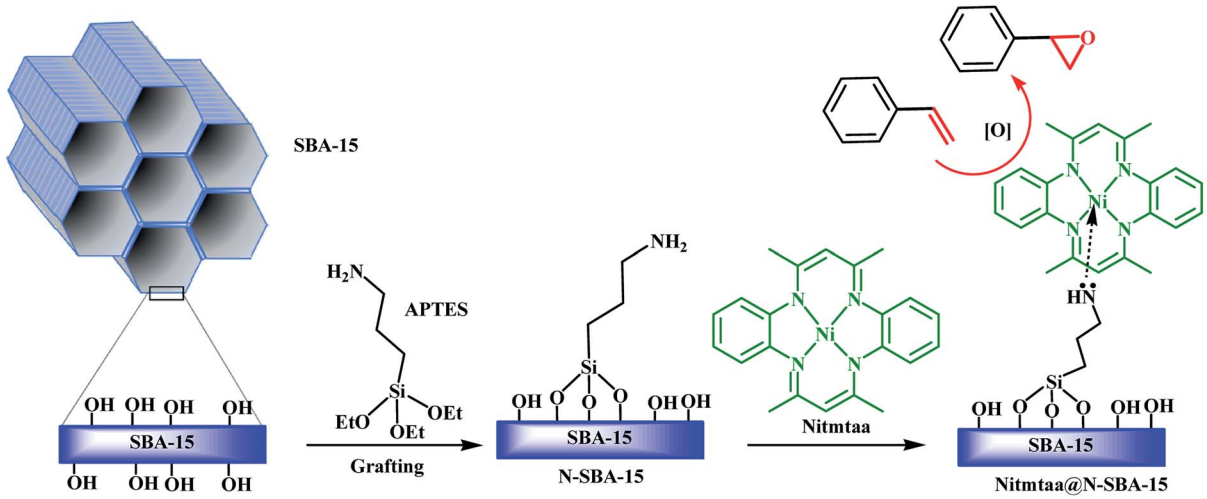

Scheme 1 Synthesis procedure of the nanocatalyst Nitmtaa@N-SBA-15.

above. The wavelength was set at a resonance line of 232.0 nm, and the spectral band pass was at 0.2 nm. A time constant of 0.2 s was used for the peak height evaluation. The air flow rate was set at 8.6 L min^{-1}, and acetylene flow rate was set at 0.8 L min^{-1}. A stock standard solution of nickel was used for the preparation of the calibration standards. The ready prepared stock solution, which was obtained from ACROS Organic, US, has concentration of 1 mg mL^{-1}. The calibration standards have concentrations of 0.1–40 mg L^{-1}.

2.3 Synthesis

2.3.1 Synthesis of amino-functionalized SBA-15 (N-SBA-15). N-SBA-15 prepared according to a procedure reported previously.[34] Briefly, in a 250 mL two-neck round-bottom flask equipped with a magnetic stirrer and a reflux condenser, 1 g of commercial SBA-15 was dispersed in 130 mL of toluene, then 0.35 mL (1.5 mmol) of APTES was added dropwise. After stirring the mixture for 15 h at 70 °C in an oil bath, the obtained product was separated by filtration, washed toughly with toluene and dried in oven at 100 °C overnight. The obtained material was labeled as N-SBA-15.

2.3.2 Synthesis of Nitmtaa@N-SBA-15. Having adapted a procedure reported in the literature,[21] a solution of 0.2 g of N-SBA-15 dispersed in 80 mL of EtOH/CH_2Cl_2 (2 : 1 v/v), was added in 250 two-neck round-bottom flask, equipped with a magnetic stirrer and a reflux condenser, then 0.1 g of Nitmtaa was added to the mixture. Nitmtaa was prepared according to a procedure published elsewhere.[35] The reaction mixture was further stirred 15 h at 50 °C. The mixture was then cooled to r.t., the product was separated by filtration, then washed thoroughly with CH_2Cl_2 to remove the excess of Nitmtaa, and dried in oven at 100 °C for 15 h to obtain the catalyst Nitmtaa@N-SBA-15 as a brown powder.

2.3.3 Styrene epoxidation. Styrene epoxidation was performed following a procedure reported by Kim *et al.*[36] and optimized later by Abboud.[43] Briefly, in a lab test tube, 15 mg of the catalyst Nitmtaa@N-SBA-15 (or 5 mg of unsupported Nitmtaa) were dispersed in 3 mL of CH_3CN/CH_2Cl_2 (1 : 1 v/v), then 60 μL (0.6 mmol) of styrene were added. After stirring this mixture at r.t. for 5 min, 156 mg of *m*-CPBA (0.9 mmol) was added, wherein the 0 time of the reaction was considered at this moment. Samples with a constant volume (30 μL) were withdrawn from the reaction mixture, filtered through hydrophobic membrane to remove the solid catalyst and then analyzed by gas chromatography (GC). Each reaction was run twice, and the average conversion and selectivity are presented.

Leaching of Nitmtaa from Nitmtaa@N-SBA-15 was measured by atomic absorption spectroscopy (AAS). In the end of each reaction, the catalyst was separated by centrifugation, and solvent of the filtrate was evaporated in the oven at 100 °C, and nickel was extracted with deionized water and measured by AAS. The remaining catalyst was reused for four cycles, and leaching measurement was performed after each cycle.

The conversion and selectivity were calculated according to the following equations:

$$\text{Conversion } (\%) = \frac{[\text{STE}]_0 - [\text{STE}]_t}{[\text{STE}]_0} \times 100$$

where $[\text{STE}]_0$ is the initial styrene concentration, $[\text{STE}]_t$ is the concentration of styrene after 5 seconds from the addition of *m*-CPBA.

$$\text{Selectivity } (\%) = \frac{[\text{STEO}]}{[\text{STE}]_0 - [\text{STE}]_t} \times 100$$

where [STEO] is the styrene oxide concentration.

The turnover frequency (TOF) was calculated according to the following equation

$$\text{TOF } (s^{-1}) = \frac{\text{moles of converted STE}}{\text{moles of Nitmtaa} \times 5 \text{ seconds}}$$

where TOF represents the number of converted moles of STE divided by the number of moles of Nitmtaa per the reaction time, which is 5 seconds.

3. Results and discussion

3.1 Synthesis and characterization

Amino-functionalized SBA-15 (N-SBA-15) was prepared according to a procedure described previously.[34] The grafting of the propyl amine groups on the surface of SBA-15 using APTES was confirmed by FT-IR (Fig. 1). The two peaks at 800 (◆) and 1044 cm^{-1} (◇) are assigned to the symmetric and asymmetric stretching vibrations of Si–O, respectively, while SiO–H bending peak (□) at around 966 cm^{-1} and SiO–H stretching broad peak (■) at around 3400 cm^{-1} in SBA-15 were disappeared in N-SBA-15, and new multiple peak at around 2974 cm^{-1} corresponding to CH_2 groups (▲) of APTES propyl chain and another small peak at around 690 cm^{-1} attributed to out-plane bending vibration of N–H (Δ) in N-SBA-15 were appeared.[21] Based on these observations, we concluded that the grafting reaction of APTES on SBA-15 was successful.

In the spectrum of Nitmtaa@N-SBA-15, the intensity of the peak of CH_2 groups (▲) at 2974 cm^{-1} increased compared to the intensity of the same peak in N-SBA-15 spectrum, this can be assigned to additional peak of CH_2 groups in Nitmtaa. Two new peaks were appeared at 1556 (○) and 1419 (●) cm^{-1} which can be attributed to the vibrations C=N and C=C in Nitmtaa, respectively.[37] Peak of N–H bending (Δ) in Nitmtaa@N-SBA-15 attributed to NH_2 groups shifted from 690 to lower frequency at 676 cm^{-1} which can be related to the coordinate bond between the lone pair electrons of NH_2 and vacant orbitals of nickel(II). Based on these findings we concluded that Nitmtaa is successfully immobilized on the surface of N-SBA-15.

Nitmtaa was prepared according to procedure described in the literature from *o*-phenylenediamine, acetylacetone and nickel acetate tetrahydrate in ethanol as a solvent.[35] Loadings of Nitmtaa in N-SBA-15 and its corresponding average surface density were determined using the atomic absorption spectrometer (Methods described above). The amount of Ni is found to be ~22 mg per 1 g of the catalyst Nitmtaa@N-SBA-15, which correspond to ~0.38 mmol of Nitmtaa per 1 g of the catalyst. The role of grafting amine groups on the surface of SBA-15 is to immobilize Nitmtaa on the surface of N-SBA-15 and prevent its leaching. A complete leaching was observed when we incorporated Nitmtaa in no-functionalized SBA-15. Total leaching of Nitmtaa from alumina was observed also by Caiut *et al.*[18]

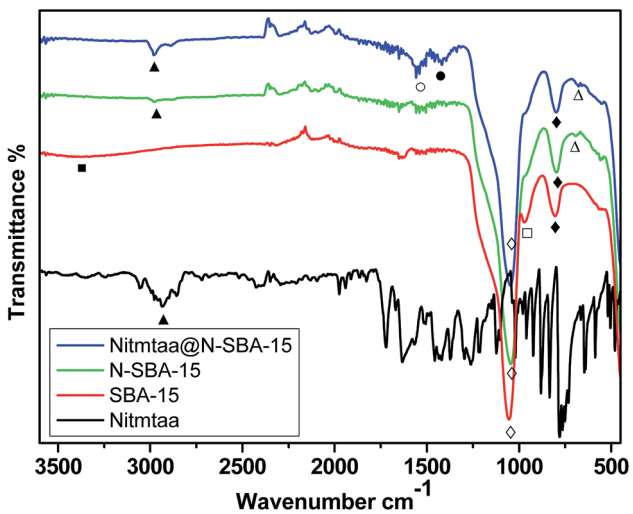

Fig. 1 FT-IR of Nitmtaa@N-SBA-15, N-SBA-15, SBA-15 and Nitmtaa. SiO–H str. [■]; CH_2 [▲]; C=N [○]; C=C [●]; Si–O [◇, ◆], SiO–H bend. [□]; N–H bend. [Δ].

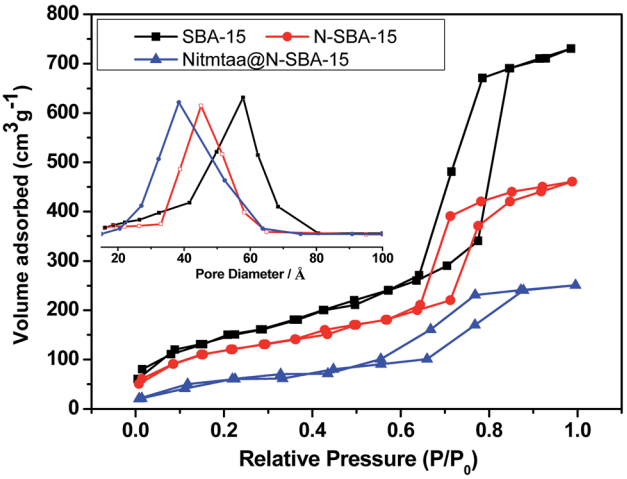

Fig. 2 N_2 adsorption/desorption isotherms and pore size distribution of Nitmtaa@N-SBA-15 and N-SBA-15.

The N_2 adsorption/desorption isotherms and pore size distributions of SBA-15, N-SBA-15, and Nitmtaa@N-SBA-15 are presented in Fig. 2. After grafting APTES in SBA-15 and addition of Nitmtaa, N_2 physisorption confirmed the preservation of the mesoporosity and framework of the obtained materials N-SBA-15 and Nitmtaa@N-SBA-15 (Fig. 2). All three materials SBA-15, N-SBA-15 and Nitmtaa@N-SBA-15 exhibited a typical IV isotherm with an H1 hysteresis loop. The BJH median pore diameter of SBA-15 was decreased from 57.9 to 45.1 Å after grafting reaction, and from 45.1 to 38.4 Å after addition of Nitmtaa (Table 1). The volumes of N_2 adsorbed by N-SBA-15 and Nitmtaa@N-SBA-15 decreased gradually, with a shift of the capillary condensation step to a lower relative pressure, due to a gradual decrease in the pore size. Compared to SBA-15, N-SBA-15 and Nitmtaa@N-SBA-15 exhibited low BET surface areas and pore volumes. All these findings confirm that APTES and Nitmtaa were successfully incorporated into SBA-15.

Fig. 3 shows the thermogravimetric analysis results of Nitmtaa@N-SBA-15, N-SBA-15 and SBA-15 samples. The weight

Table 1 Textural properties of Nitmtaa@N-SBA-15, N-SBA-15 and SBA-15

Samples	S_{BET} ($m^2\ g^{-1}$)	Pore diameter[a] (Å)	Pore volume ($cm^3\ g^{-1}$)
SBA-15	633	57.9	0.68
N-SBA-15	367	45.1	0.59
Nitmtaa@N-SBA-15	252	38.4	0.41

[a] Calculated from BJH adsorption branch.

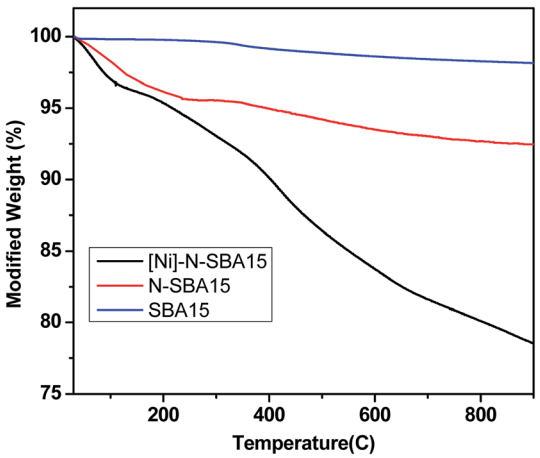

Fig. 3 Thermogravimetry analysis of Nitmtaa@N-SBA-15, N-SBA-15 and N-SBA-15 in air stream.

loss observed below 200 °C is related to the physically adsorbed H_2O, which present about 5%. Propylamine groups of N-SBA decompose between 330 °C and 450 °C, with a weight loss of around 5%, and the weight loss observed up to 850 °C could be attributed to the condensation reaction between silanol groups of silica.[38,39] In this respect, about 3.5% weight loss of N-SBA-15 is related to the decomposition of APTES. We can conclude from this result that for 1 g of N-SBA-15 ~1.0 mmol APTES is grafted.

Also, the TGA analysis of Nitmtaa@N-SBA-15 was investigated. Thermogravimetric analysis of pure Nitmtaa, reported previously,[40] shows two steps, first step from 240 °C to 340 °C related to the decomposition of substituents (-CH_3), and a second weight loss step was observed from 340 °C to 480 °C which attributed to the decomposition of the tetraazaannulene ring (tmtaa). However, the thermal stability of Nitmtaa is expected to be improved if it is incorporated in a solid matrix.[40] The mass-loss in Nitmtaa@N-SBA-15 thermogram continued until 750 °C which indicate the high thermal stability of the supported Nitmtaa at high temperature. The weight loss attributed to the decomposition of the ligand tmtaa is about 13.8% which correspond ~160 mg (0.40 mmol) of Nitmtaa per 1 g of the catalyst. This is in agreement with the amount of Nitmtaa per 1 g of the catalyst determined by AAS which is at ~0.38 mmol.

The morphology of Nitmtaa@N-SBA-15 and N-SBA-15 is shown in Fig. 4. The SEM images of N-SBA-15 (a and d), and Nitmtaa@N-SBA-15 (c and d) depict a worm-like particles with length ranging 0.5–5.0 μm and 0.5–2.0 μm, respectively. N-SBA-15 particles show some degree of aggregation with the formation of tubular agglomerates with different length (5–70 μm) (Fig. 4a and b). The aggregation of N-SBA-15 can be attributed to formation of hydrogen bonds in propylamine chains layer formed around the particles.[41] After the addition of Nitmtaa to N-SBA-15, the aggregation degree decreased dramatically and the big tubular agglomerates observed in N-SBA-5 disappeared

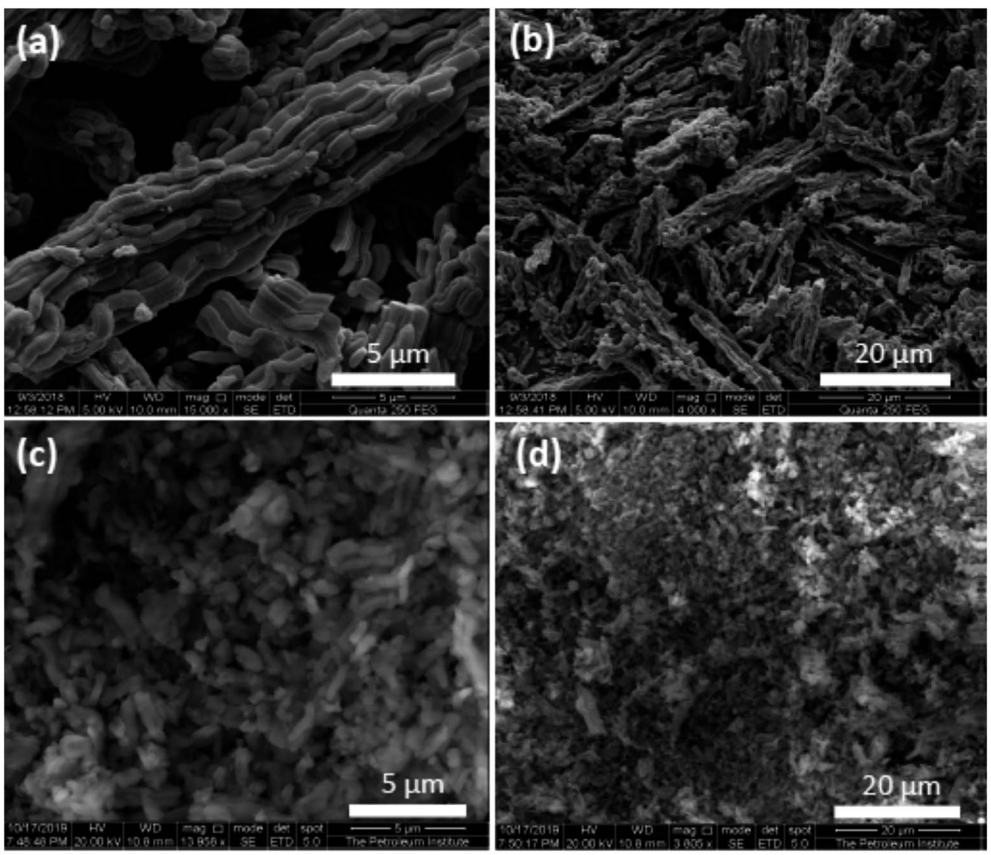

Fig. 4 SEM images of N-SBA-15 (a and b) and Nitmtaa@N-SBA-15 (c and d).

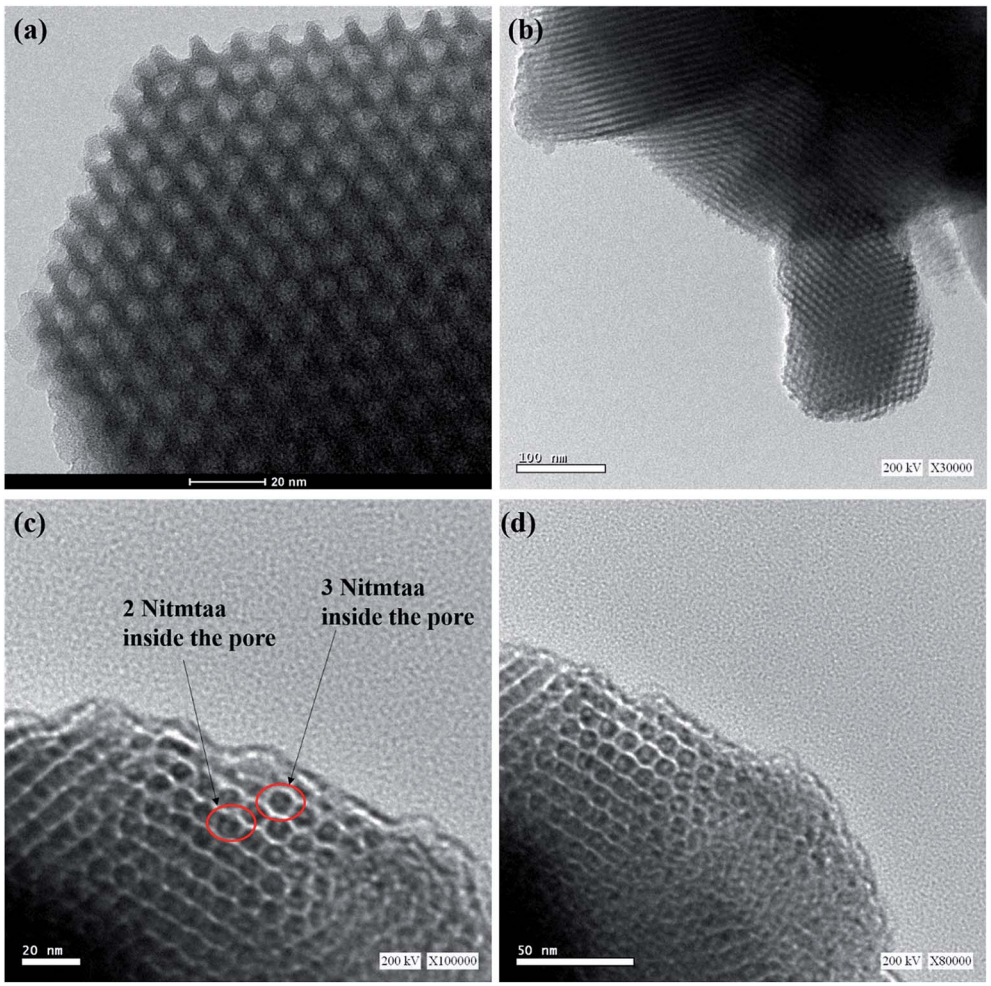

Fig. 5 TEM images of N-SBA-15 (a) and Nitmtaa@N-SBA-15 (b–d).

with the appearance of isolated small particles (Fig. 4d), this is probably due to the coordination of Nitmtaa with amine groups in the surface of N-SBA-5 which led to the stabilization of silica particles.

Fig. 5 shows TEM images of N-SBA-15 and Nitmtaa@N-SBA-15. Enlarged TEM images of both materials depict a long-range order of uniform pores with a perpendicular view, and illustrates clearly the honey-comb like hexagonal mesopores. Despite the change appeared in their microscopic morphology (Fig. 4), these images confirm that the structural integrity of the silica matrix has been preserved after the grafting of APTES into silica framework and the coordination of Nitmtaa. Enlarged TEM images of Nitmtaa@N-SBA-15 (Fig. 5b–d) shows clearly a uniform distribution of Nitmtaa (black spots) into silica pores, with 2 to 3 molecules of Nitmtaa in the corners of each hexagonal mesopore (see red cycle in Fig. 5c).

Powder XRD was performed for samples N-SBA-15 and Nitmtaa@N-SBA-15 to investigate the dispersion of Nitmtaa through silica framework. Fig. 6 present XRD patterns of N-SBA-15 and Nitmtaa@N-SBA-15. Both samples exhibited only one broad peak at around $2\theta = 22.9°$ which is a characteristic signal of amorphous silica material.[42] As expected, the absence of any crystalline phase indicates that Nitmtaa is highly dispersed through N-SBA-15 framework, and only Nitmtaa molecules coordinated to the isolated NH_2 groups are present in the material.

3.2 Styrene epoxidation

The catalytic performance of the new synthesized nanocatalyst Nitmtaa@N-SBA-15 was evaluated in the epoxidation of styrene, using *m*-CPBA as an oxygen donor, in CH_2Cl_2/CH_3CN (1 : 1 v/v) as solvent under ambient conditions (22 °C, 1 atm), following an optimized procedure described previously by Abboud[43] for the flower-like mesoporous NiO NPs, and by Hamdy *et al.* for Ni-TUD-1.[33] When 1.5 equivalent (eq.) of *m*-CPBA was added to the reaction mixture in the presence of 10 mg of Nitmtaa@N-SBA-15, an immediate reaction took place. Due to the notable fast reaction, sample was withdrawn after only 5 seconds, filtered and sent directly to GC for analysis.

Table 2 lists the styrene conversion and selectivity towards the formed epoxide obtained with the nanocatalyst Nitmtaa@N-SBA-15 compared to the obtained results of other Ni-based catalysts and other catalysts reported in the literature. First, no conversion was observed without the addition of the catalyst

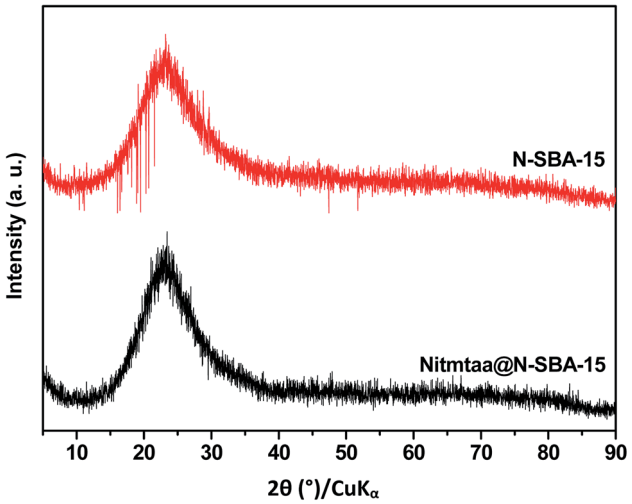

Fig. 6 XRD patterns of N-SBA-15 and Nitmtaa@N-SBA-15.

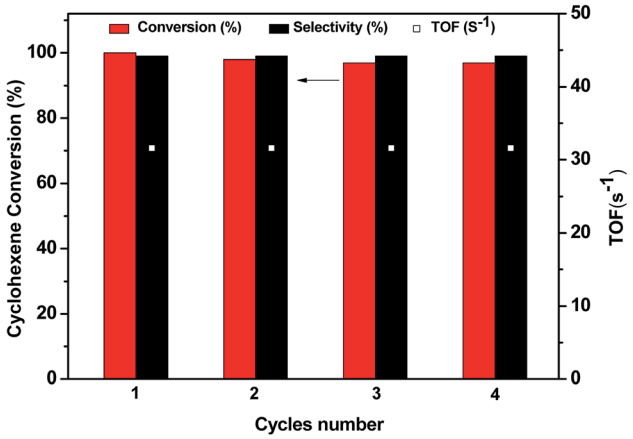

Fig. 7 Recycling study of the nanocatalyst Nitmtaa@N-SBA-15 in the epoxidation of styrene with *m*-CPBA for four runs.

(entry 1). This is an indication for the need of a catalyst to perform the oxidation of styrene even in the presence of the strong oxidant such as *m*-CPBA. In the presence of bulk NiO, 62% of styrene was converted, with a selectivity of 68% towards styrene oxide (desired product) and a TOF of 0.53 s^{-1} (entry 2). To avoid the aggregation and low stability of NiO NPs, our catalytic group prepared an efficient catalyst based on the incorporation of 5 wt% NiO NPs in SBA-15 mesoporous material according to the work reported by Cheng *et al.*[44] Ni-SBA-15 exhibited high activity in which 100% conversion of styrene with 93% selectivity towards styrene oxide was obtained instantly with TOF around 5.97 s^{-1} (entry 3). However, Ni-SBA-15 showed a poor stability, whereas, after the first run around 12% of Ni ions were detected in the reaction solution. These results proved that Ni^{2+} ions are not strongly bonded to SBA-15 channels and can be partially removed from the framework during the epoxidation reaction. In contrast, Nitmtaa@N-SBA-15 exhibited a quantitative conversion of styrene to styrene oxide, with high stability and high TOF ~31.58 s^{-1} (entry 4). After 4 runs, Nitmtaa@N-SBA-15 exhibited a quasi-constant catalytic activity and TOF with negligible leaching (Fig. 7). The styrene conversion in the four runs and the selectivity towards styrene oxide are almost the same. This is a strong evidence for the high reusability of the Nitmtaa@N-SBA-15 catalyst.

A comparison of the catalytic activity of Nitmtaa@N-SBA-15 in the epoxidation reaction of styrene with other catalysts reported in the literature is listed in Table 2 (entries 5–12). These selected catalysts are among the most efficient catalysts used for the epoxidation of styrene. This list includes mesoporous materials supported metallic, bimetallic and OTMC systems. We can notice that the Nitmtaa@N-SBA-15 catalyst provides a quantitative conversion of styrene to cyclohexene immediately at room temperature which is much better than all reported catalysts.[45–52] While, heat at around 80 °C with prolonged reaction time (≥6 h).

As mentioned above, the recycling of the Nitmtaa@N-SBA-15 catalyst was investigated through performing the epoxidation of styrene for four consecutive cycles without further treatment in the catalyst. Two methods were applied to separate the solid

Table 2 Styrene epoxidation performance over Nitmtaa@N-SBA-15 compared to some blanks and other catalysts reported in the literature

Entry	Catalyst	*T* (°C)	Time (h)	ST conversion (%)	STO selectivity (%)
1	None[a]	22	24	0	0
2	NiO	22	<1 min	62	68
3	Ni-SBA-15	22	<1 min	100	95
4	Nitmtaa@N-SBA-15	22	<1 min	100	99
5 (ref. 45)	Au/BaTNT	80	15	80	65
6 (ref. 46)	Ag/SBA-15	80	24	78	47
7 (ref. 47)	Cu salen@MOF	80	6	99	89
8 (ref. 48)	Cu_7Co_3/AHS	80	6	65	93
9 (ref. 49)	CuO/CoAl-HT	85	6	99	72
10 (ref. 50)	Cobalt(cyclam)/SBA-15	40	12	60	40
11 (ref. 51)	VO(acac:8-Q)-SBA-15	80	8	91	50
12 (ref. 52)	Co-MCM-41	80	24	50	45

[a] Reaction conditions: 10 mg of catalyst (5 mg for NiO), 0.06 mL of styrene, 156 mg of *m*-CPBA (1.5 eq.), 3 mL of solvent: CH_3CN/CH_2Cl_2 (1 : 1 v/v), *T* = ~22 °C, 1 atm.

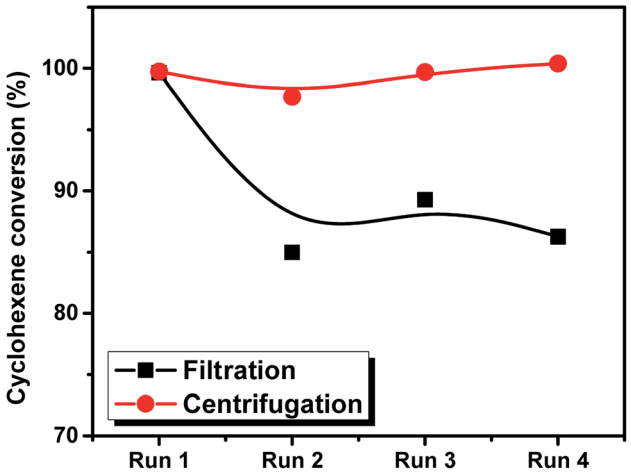

Fig. 8 The conversion of styrene as a function of four consecutive reactions by using to separation methods; filtration and centrifugation.

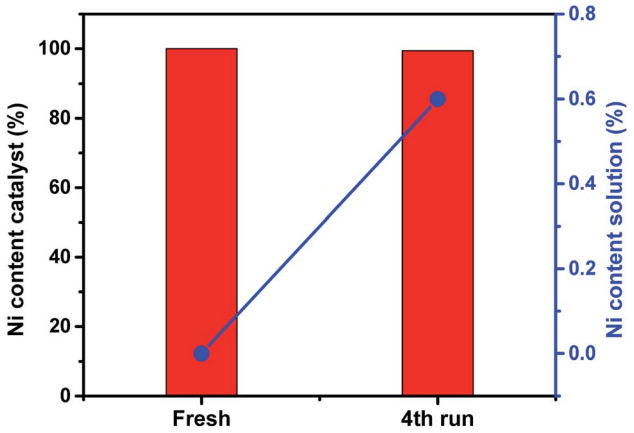

Fig. 9 The amount of Ni (%) either in the catalyst of in the reaction medium before and after the four runs as determined from flame photometer.

catalyst from the reaction medium; centrifugation and filtration. The obtained styrene conversion % for the Nitmtaa@N-SBA-15 obtained by the two methods is presented in Fig. 8. It was clearly observed that the conversion in the case of filtration is decreasing with the running reactions, however in the case of centrifugation, the styrene conversion was found to be almost the same. Through filtration, and due to the small amount of the applied catalyst, a small effective amount of the catalyst was lost and therefore, the conversion was decreased from 100% in the first run to 92% after the fourth run. On the other hand, by using centrifugation method, the whole amount of the catalyst was kept in the reactor, almost no loss in activity was observed. This is an additional proof for the high stability of the prepared catalyst.

The amount of Ni ions were quantified in the solution and in the solid catalyst after digestion by using flame photometer technique. This analysis was performed in order to explore leachning of Ni out of the complex or complex leaching from the silica framework. The measured Ni contents (%) in the solid catalyst and the reaction medium after the fourth run are plotted in Fig. 9. The results show that only 0.6% of Ni active sites were leached from the solid catalyst and were found in the reaction medium. This result indicates the high stability of the active sites and the minimum leaching property of the prepared catalyst and therefore the superior activity which last for four continuous reaction without activity loss.

Based on the obtained results, the styrene conversion is increased from NiO NPs to Ni-SBA-15 because of the high surface area of Ni-SBA-15. Moreover, the TOF is increased dramatically, this can be attributed (the amount of catalyst kept constant) to the small amount of Ni present in SBA-15 and since, the TOF was also increased sharply when Nitmtaa@N-SBA-15 is used due to the perfect dispersion of the active sites into the SBA-15 and also due to the decrease of Ni content than Ni-SBA-15. Moreover, the high stability of Nitmtaa@N-SBA-15 recommend the testing of this catalyst in the second level (semi-pilot batch reactor) of the industrial epoxidation process.

3.3 Proposed mechanism

Based on previous mechanistic investigations, trapping experiments and theoretical studies of the epoxidation reactions of olefins catalysed by organometallic complexes of late transition metals, *e.g.* Fe, Cr, Ru, Mn, Ni, with facilely accessible high oxidation states, include porphyrin transition metal complexes, and using peroxycarboxylic acids such as *m*-CPBA as oxygen donor, this reaction probably operates by redox mechanism involving the formation of Ni^{II}-OOAr and Ni-Oxo activated species, which transfer the oxygen to the olefin either directly or by the intermediacy of a metallacycle, a radical, cation species, or *via* concerted transition state.[10,49,53,54]

For porphyrins complexes, this mechanism was named by Groves as oxygen-rebound mechanism.[55] In this mechanism, an oxygen atom is transferred from the oxidant to the metal ion to form metal-oxo species (M-Oxo) with high oxidation state, which in turn transfers this oxygen atom to the olefinic substrate.[10,36,56–58]

Therefore, the following reaction pathway (Fig. 10) has been proposed for the epoxidation reaction of styrene over the prepared nanocatalyst Nitmtaa@N-SBA-15 using *m*-CPBA as oxygen donor.

As shown in Fig. 10, the reaction starts by the immediate adsorption of *m*-CPBA on the surface of Nitmtaa@N-SBA-15, followed by deprotonation of *m*-CPBA and formation of nickel-bonded-*m*-CPBA (Ni^{II}-OOAr, (A)). Based on the literature, in aprotic solvents, tree pathways are possible for the cleavage of O–O bond: heterolysis, homolysis or direct epoxidation.[10,53] It is well known that O–O bond in peracids cleaves heterolytically.[59–63] Groves and Traylor have proposed that the M-Oxo forms by heterolysis.[57,64–66] The O–O cleavage was also approved to be affected by the type of the oxidant, whereas the tendency of O–O heterolysis is in the following order: *m*-CPBA > H_2O_2 > *t*-BuOOH. According to these results the O–O in Ni^{II}-OOAr bond would cleave heterotically to form the activated Ni^{IV}-Oxo (B), accompanied with a proton transfer to assist the formation of *meta*-chlorobenzoic acid (*m*-CBA).

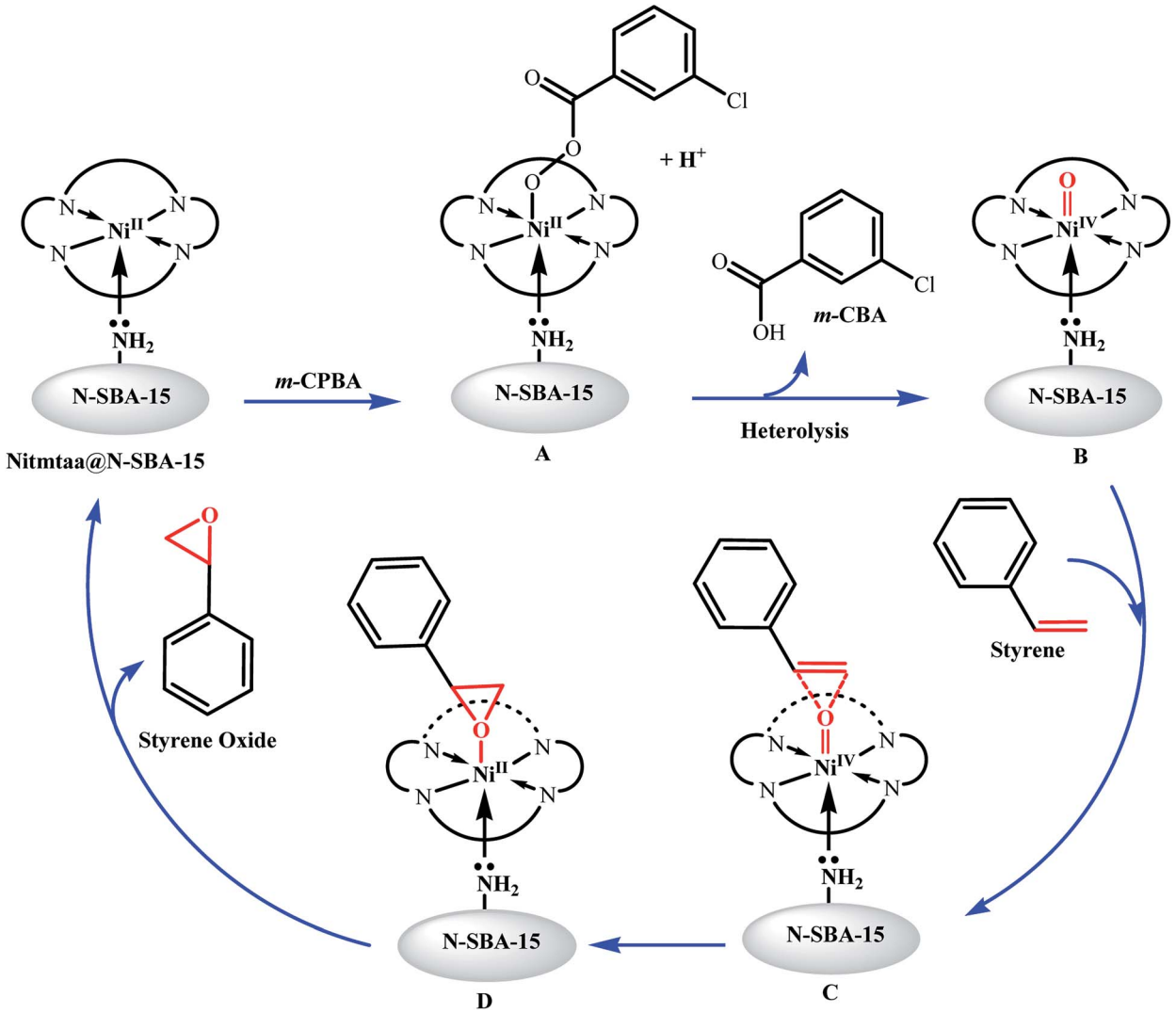

Fig. 10 Concerted transition state pathway for the epoxidation of styrene over Nitmtaa@N-SBA-15.

The addition of *m*-CPBA to the reaction mixture led to a spontaneous change in colour of the solution from brown to yellow due to the *in situ* formation of the corresponding Ni^{IV}-Oxo (B).[67] Similar observation was reported by Kaim *et al.* during the epoxidation of styrene catalyzed by a ruthenium(II) organometallic complex.[54]

The electrophilic nickel-oxo intermediate Ni^{IV}-Oxo thereafter interacts with styrene with eventual transfer of the oxygen atom to the double bond. It has been proposed previously that this transfer of the oxo group can proceed *via* different possible pathways, such as concerted transition state, metalaoxetane, carbon radical, π-radical cation or carbocation.[54,68–70]

Based on DFT calculations and NMR analysis, Kaim *et al.* confirmed that the concerted transition state pathway is the most likely.[54] Therefore, we suggest that the transfer of the oxygen atom form Ni^{IV}-Oxo to the styrene can proceed *via* the concerted transition state C, then the styrene oxide (the desired product) is formed by the cleavage of the intermediate (D), and the catalyst Nitmtaa@N-SBA-15 is recovered.

However, based on previous mechanistic studies performed on late TM porphyrins complexes, a second pathway can take place also in parallel with the concerted transition state pathway, which is the direct epoxidation of styrene by the Lewis acid mechanism (Fig. 11).[71–74] It is reported that Ni^{II}-OOAr in aprotic solvents can undergo a direct epoxidation reaction.[53] In addition, Ni^{II} active sites in Nitmtaa@N-SBA-15 catalyst are electron-poor metal centers, and would increase the proximal oxygen electrophilicity in N^{II}-OOAr peroxide, making this complex an efficient oxygen-transfer agent. The nucleophilic attack of C=C double bond of the styrene on the proximal oxygen atom of the peroxy complex N^{II}-OOAr leads to the formation of the concerted transition state (E). After the breakage of (E), the styrene oxide is formed, and the starting catalyst Nitmtaa@N-SBA-15 is recovered.

4. Conclusion

New and efficient nanocatalyst, named Nitmtaa@N-SBA-15, was successfully synthesised by immobilizing Nitmtaa complex on

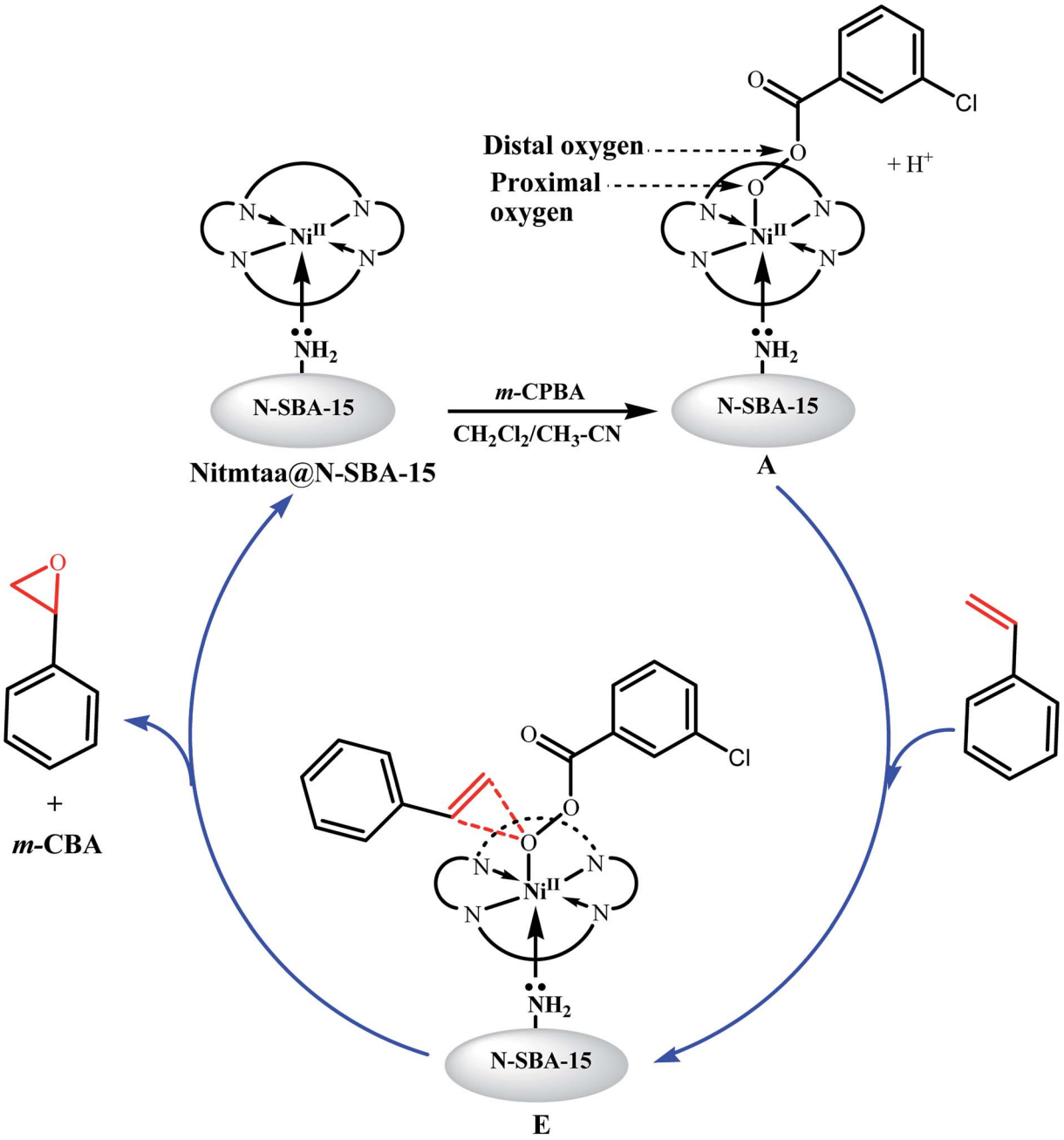

Fig. 11 Direct epoxidation of styrene over Nitmtaa@N-SBA-15.

amino-functionalized SBA-15 *via* coordinate bond between nickel atom and NH_2 group. The successful grafting of APTES in SBA-15 surface and the coordination of Nitmtaa were confirmed by FT-IR and BET. N_2 physisorption confirmed the preservation of the mesoporosity and framework of the obtained nanocatalyst Nitmtaa@N-SBA-15, with decreases in surface, pore diameter and pore volume because of the coordination of Nitmtaa inside the pores of SBA-15. TEM and XRD characterizations revealed a high dispersion of Nitmtaa complex in SBA-15 pores. TGA analysis displayed a high thermal stability of the obtained material. The prepared Nitmtaa@N-SBA-15 nanocatalyst exhibited a high catalytic activity performance toward the epoxidation of styrene. An immediate and quantitative conversion of styrene to styrene oxide with a high turnover frequency of ~31.58 s^{-1} was obtained under ambient conditions using *m*-CPBA as an oxidant. Moreover, the new nanocatalyst Nitmtaa@N-SBA-15 exhibited a quasi-constant catalytic activity performance and high stability in four successive reused cycles. Leaching measurement using atomic absorption spectroscopy (AAS) confirmed a high stability of nanocatalyst. Plausible reaction mechanism pathways are also proposed.

Conflicts of interest

There are no conflicts to declare.

Acknowledgements

The authors acknowledge the Deanship of Scientific Research at King Khalid University for funding this work through a research group project number R.G.P1/89/40. Moreover, the authors also extend their appreciation to the Deanship of Scientific Research at King Saud University for funding this work through research group no. (RG-1440-141).

References

1 K. Kamata, K. Yonehara, Y. Sumida, K. Yamaguchi, S. Hikichi and N. Mizuno, *Science*, 2003, **300**, 964–966.
2 C. D. Nunes, P. D. Vaz, V. Felix, L. F. Veiros, T. Moniz, M. Rangel, S. Realista, A. C. Mourato and M. J. Calhorda, *Dalton Trans.*, 2015, **44**, 5125–5138.
3 L. Y. Hu, B. Yue, C. Wang, X. Y. Chen and H. Y. He, *Appl. Catal., A*, 2014, **477**, 141–146.
4 L. J. Davies, P. McMorn, D. Bethell, P. C. B. Page, F. King, F. E. Hancock and G. J. Hutchings, *J. Catal.*, 2001, **198**, 319–327.
5 G. D. Yadav and Y. S. Lawate, *Ind. Eng. Chem. Res.*, 2013, **52**, 4027–4039.
6 (*a*) J. Sebastian, K. Jinka and R. Jasra, *J. Catal.*, 2006, **244**, 208–218; (*b*) G. Xu, Q. H. Xia, X. H. Lu, Q. Zhang and H. J. Zhan, *J. Mol. Catal. Chem.*, 2007, **266**, 180–187.
7 M. S. Batra, R. Dwivedi and R. Prasad, *ChemistrySelect*, 2019, **4**, 11636–11673.
8 N. Ananthi and I. V. M. V. Enoch, *Chirality*, 2019, **31**, 155–163.
9 W. Dai, G. Li, B. Chen, L. Wang and S. Gao, *Org. Lett.*, 2015, **17**, 904–907.
10 S. Ted Oyama, *Mechanisms in Homogeneous and heterogeneous Epoxidation Catalysis*, Elsevier, Oxford, 1st edn, 2008.
11 J. Eilmes, *Polyhedron*, 1991, **10**, 1779.
12 J. D. Koola and J. K. Kochi, *Inorg. Chem.*, 1987, **26**, 908–916.
13 S. Storck, H. Bretinger and W. F. Maier, *Appl. Catal., A*, 1998, **174**, 137.
14 R. W. Lee, P. C. Nakagaki and T. C. Bruice, *J. Am. Chem. Soc.*, 1989, **111**, 1368.
15 E. G. Jaeger, *Z. Anorg. Allg. Chem.*, 1969, **364**, 177.
16 V. L. Goedken, J. Molin Case and Y.-A. Whang, *J. Chem. Soc., Chem. Commun.*, 1973, 337–338.
17 V. L. Goedken, J. J. Pluth, S.-M. Peng and B. Bursten, *J. Am. Chem. Soc.*, 1976, **98**, 8014.
18 J. M. A. Caiut, S. Nakagaki, O. J. De Lima, C. Mello, C. A. P. Leite, E. J. Nassar, K. J. Ciuffi and H. C. Sacco, *J. Sol-Gel Sci. Technol.*, 2003, **28**, 57–64.
19 E. M. Serwicka, J. Poltowicz, K. Bahranowski and Z. Olejniczak, *Appl. Catal., A*, 2004, **275**, 9–14.
20 S. Farahmand and M. Ghiaci, *Microporous Mesoporous Mater.*, 2019, **288**, 109560.
21 F. Yang, S. Gao, C. Xiong, H. Wang, J. Chen and Y. Kong, *Chin. J. Catal.*, 2015, **36**, 1035–1041.
22 E. A. Prasetyanto and S.-E. Park, *Bull. Korean Chem. Soc.*, 2008, **29**, 1033–1037.
23 S. Y. Lim, M. Kang, J. M. Kim and I. M. Lee, *Bull. Korean Chem. Soc.*, 2005, **26**, 887–891.
24 S. Seelan and A. K. Sinha, *Appl. Catal., A*, 2003, **238**, 201–209.
25 E. Blaz and J. Pielichowski, *Molecules*, 2006, **11**, 115–120.
26 K. Parida and G. B. B. Varadwaj, *Ind. Eng. Chem. Res.*, 2011, **50**, 7849–7856.
27 G. B. B. Varadwaj and S. Sahu, *Ind. Eng. Chem. Res.*, 2011, **50**, 8973–8982.
28 D. Gournis and M. Louloudi, *Mater. Sci. Eng., C*, 2002, **22**, 113–116.
29 M. Salavati-Niasari, *J. Mol. Catal. A: Chem.*, 2007, **263**, 247–252.
30 S. Campestrini and B. Meunier, *Inorg. Chem.*, 1992, **31**, 1999–2004.
31 Y. L. Ye, M. Jin and D. C. Wan, *J. Mater. Chem. A*, 2015, **3**, 13519–13525.
32 S. J. Pierre, J. C. Thies, A. Dureault, N. R. Cameron, J. C. M. van Hest, N. Carette, T. Michon and R. Weberskirch, *Adv. Mater.*, 2006, **18**, 1822–1826.
33 M. S. Hamdy, *et al.*, *Catal. Lett.*, 2020, in revision.
34 M. Abboud, T. Sahlabji, M. Abu Haija, A. A. El-Zahhar, S. Bondock, I. Ismail and S. M. A. S. Keshk, *New J. Chem.*, 2020, **44**, 2291–2302.
35 Y. Y. Shen, M. Q. Zhu, J. P. Du, Y. Y. Yang and Y. Tang, *Adv. Mater. Res.*, 2011, **396–398**, 1699–1702.
36 K. H. Bok, M. M. Lee, G. R. You, H. M. Ahn, K. Y. Ryu, S.-J. Kim and C. Kim, *Chem.–Eur. J.*, 2017, **23**, 3117–3125.
37 Q. Q. Zhu, S. Maeno, R. Nishimoto, T. Miyamoto and M. Fukushima, *J. Mol. Catal. A: Chem.*, 2014, **385**, 31.
38 M. Espinosa, S. Pacheco and R. Rodriguez, *J. Non-Cryst. Solids*, 2007, **353**, 2573–2581.
39 M. Moritz and M. Łaniecki, *Appl. Surf. Sci.*, 2012, **258**, 7523–7529.
40 E. V. Basiuk, M. Martínez-Herrera, E. Álvarez-Zauco, L. V. Henao-Holguín, I. Puente-Lee and V. A. Basiuk, *Dalton Trans.*, 2014, **43**, 7413–7428.
41 A. F. M. Pinheiro, A. Nijmeijer, V. G. P. Sripathi and L. Winnubst, *Eur. J. Chem.*, 2015, **6**, 287–295.
42 F. Adam, T.-S. Chew and J. Andas, *J. Sol-Gel Sci. Technol.*, 2011, **59**, 580–583.
43 M. Abboud, *React. Kinet., Mech. Catal.*, 2020, DOI: 10.1007/s11144-020-01864-y.
44 M.-Y. Cheng, C.-J. Pan and B.-J. Hwang, *J. Mater. Chem.*, 2009, **19**, 5193–5200.
45 D. Nepak and D. Srinivas, *Appl. Catal., A*, 2016, **523**, 61–72.
46 X. Huang, W. Dong, G. Wang, M. Yang, L. Tan, Y. Feng and X. Zhang, *J. Colloid Interface Sci.*, 2011, **359**, 40–46.
47 K. Huang, L. Guo and D. Wu, *Ind. Eng. Chem. Res.*, 2019, **58**, 4744–4754.
48 B. Li, J. Huang and X. Wang, *Chem. Res. Chin. Univ.*, 2018, **35**, 125–132.
49 R. Hu, P. Yang, Y. Pan, Y. Li, Y. He, J. Feng and D. Li, *Dalton Trans.*, 2017, **46**, 13463–13471.
50 S. Eko, A. Prasetyanto, S. C. Han and S. E. Park, *J. Korean Chem. Soc.*, 2006, **27**, 1381–1385.
51 Z. Li, L. Liu, J. Hu, H. Liu, S. Wu, Q. Huo, J. Guan and Q. Kan, *Appl. Organomet. Chem.*, 2012, **26**, 252–257.

52 S. Bhunia, S. Jana, D. Saha, B. Dutta and S. Koner, *Catal. Sci. Technol.*, 2014, **4**, 1820–1828.
53 H. M. Ahn, J. M. Bae, M. J. Kim, K. H. Bok, H. Y. Jeong, S. J. Lee and C. Kim, *Chem. - Eur. J.*, 2017, **23**, 11969–11976.
54 H. Agarwala, F. Ehret, A. D. Chowdhury, S. Maji, S. M. Mobin, W. Kaim and G. K. Lahiri, *Dalton Trans.*, 2013, **42**, 3721.
55 J. T. Groves, *J. Chem. Educ.*, 1985, **65**, 928.
56 A. Murphy, G. Dubois and T. D. P. Stack, *J. Am. Chem. Soc.*, 2003, **125**, 5250.
57 T. G. Traylor, S. Tsuchiya, Y. S. Byun and C. Kim, *J. Am. Chem. Soc.*, 1993, **115**, 2775.
58 J. M. Garrison and T. C. Bruice, *J. Am. Chem. Soc.*, 1989, **111**, 191.
59 J. T. Groves, R. C. Haushalter, M. Nakamura, T. E. Nemo and B. J. Evans, *J. Am. Chem. Soc.*, 1981, **103**, 2884.
60 J. T. Groves and Y. Watanabe, *J. Am. Chem. Soc.*, 1986, **108**, 7834.
61 J. T. Groves and Y. Watanabe, *J. Am. Chem. Soc.*, 1988, **110**, 8443.
62 T. G. Traylor, W. A. Lee and D. V. Stynes, *J. Am. Chem. Soc.*, 1984, **106**, 755.
63 W. A. Lee and T. C. Bruice, *J. Am. Chem. Soc.*, 1985, **107**, 513.
64 T. G. Traylor, C. Kim, J. L. Richards, F. Xu and C. L. Perrin, *J. Am. Chem. Soc.*, 1995, **117**, 3468.
65 T. G. Traylor, W.-P. Fann and D. Bandyopadhyay, *J. Am. Chem. Soc.*, 1989, **111**, 8009.
66 T. G. Traylor, C. Kim, W.-P. Fann and C. L. Perrin, *Tetrahedron*, 1998, **54**, 7977.
67 E. Andris, R. Navratil, J. Jasik, M. Srnec, M. Rodriguez, M. Costas and J. Roithová, *Angew. Chem., Int. Ed.*, 2019, **58**, 9619–9624.
68 A. D. Chowdhury, A. Das, K. Irshad, S. M. Mobin and G. K. Lahiri, *Inorg. Chem.*, 2011, **50**, 1775.
69 D. Ostovic and T. C. Bruice, *Acc. Chem. Res.*, 1992, **25**, 314.
70 W.-H. Fung, W.-Y. Yu and C.-M. Che, *J. Org. Chem.*, 1998, **63**, 7715.
71 W. Nam, H. J. Han, S.-Y. Oh, Y. J. Lee, M.-H. Choi, S.-Y. Han, C. Kim, S. K. Woo and W. Shin, *J. Am. Chem. Soc.*, 2000, **122**, 8677.
72 W. Nam, M. H. Lim, H. J. Lee and C. Kim, *J. Am. Chem. Soc.*, 2000, **122**, 6641.
73 W. Nam, M. H. Lim, S. K. Moon and C. Kim, *J. Am. Chem. Soc.*, 2000, **122**, 10805.
74 W. Nam, M. H. Lim, S.-Y. Oh, J. H. Lee, S. K. Woo, C. Kim and W. Shin, *Angew. Chem., Int. Ed. Engl.*, 2000, **39**, 3646.

